Research paper

Origin of crude oils from oilfields in the Zagros Fold Belt, southern Iraq: Relation to organic matter input and paleoenvironmental conditions

Mohammed Hail Hakimi [a,*], Ahmed Askar Najaf [b]

[a] Geology Department, Faculty of Applied Science, Taiz University, 6803 Taiz, Yemen
[b] College of Geophysics and Remote Sensing, Al-Karkh University, Iraq

ABSTRACT

Crude oil samples from Cretaceous and Tertiary reservoir sections in the Zagros Fold Belt oil fields, southern Iraq were investigated using non-biomarker and biomarker parameters. The results of this study have been used to assess source of organic matter, and the genetic link between oils and their potential source rocks in the basin. The oils are characterized by high sulphur and trace metal (Ni, V) contents and relatively low API gravity values ($17.4-22.7°$ API). This indicates that these oils are heavy and generated from a marine source rock containing Type II-S kerogen. This is supported by their biomarker distributions of normal alkanes, regular isoprenoids, terpanes and steranes and the bulk carbon isotope compositions of their saturated and aromatic hydrocarbons. The oils are characterized by low Pr/Ph ratios (<1), high values of the C_{35} homohopane index and C_{31}-22R/C_{30} hopane ratios, relatively high C_{27} sterane concentrations, and the predominance of C_{29}-norhopane. These biomarkers suggest that the oils were generated predominantly from a marine carbonate source rock, deposited under reducing conditions and containing plankton/algal and microorganisms source input. The presence of gamma-cerane also suggests water column stratification during source rock deposition.

The biomarker characteristics of the oils are consistent with those of the Middle Jurassic Sargelu carbonate as the effective source rock in the basin. Biomarker maturity data indicate that the oils were generated from early maturity source rocks.

© 2016 Elsevier Ltd. All rights reserved.

1. Introduction

The Zagros Fold Belt and Mesopotamian Basin are the main basins in Iraq, extending from northern to southern Iraq (Fig. 1). These two Iraqi basins have large oil and gas reserves contained in giant oilfields (Al-Sakini, 1992; Sadooni, 1993, Sadooni and Aqrawi, 2000) as defined by Bally and Snelson (1980).

The area of interest of this study lies in the southern part of the Zagros Fold Belt (Fig. 1). The Zagros Fold Belt is an important hydrocarbon province in Iraq and contains several, well known hydrocarbon fields (Fig. 1a). The Zagros Fold Belt has attracted the interest of numerous researchers and oil companies (e.g., Al-Ahmed, 2006; Al-Ameri and Zumberge, 2012; Mohialdeen et al., 2013; Al-Ameri et al., 2013; Sachsenhofer et al., 2015). All of these

prior publications have studied the northern part of the Zagros Fold Belt. These studies report the presence of possible source rocks occurring within the Jurassic to Cretaceous rock units. These potential source rocks are the Upper Jurassic-Lower Cretaceous Chia Gara, Upper Jurassic Naokelekan and Middle Jurassic Sargelu formations. The Jurassic—Lower Cretaceous source rocks of the northern part of Zagros Fold Belt are bituminous limestones and black shales, which have high total organic carbon (TOC) contents ranging from 2 to 20 wt%. These source rocks all contain high sulphur-rich (Mohialdeen et al., 2013; Sachsenhofer et al., 2015), and suggests the presence of Type II-S kerogen, which can be expected to generate early-mature sulphur-rich oils (Baskin and Peters, 1992). These source rocks were deposited in a carbonate-rich, anoxic environment with elevated salinity (Mohialdeen et al., 2013; Al-Ameri et al., 2014; Sachsenhofer et al., 2015). However, little is known about the quality and maturity of the potential source rocks or about the oil characteristic accumulated in the southern part of the Zagros. In this regard, eleven crude oil
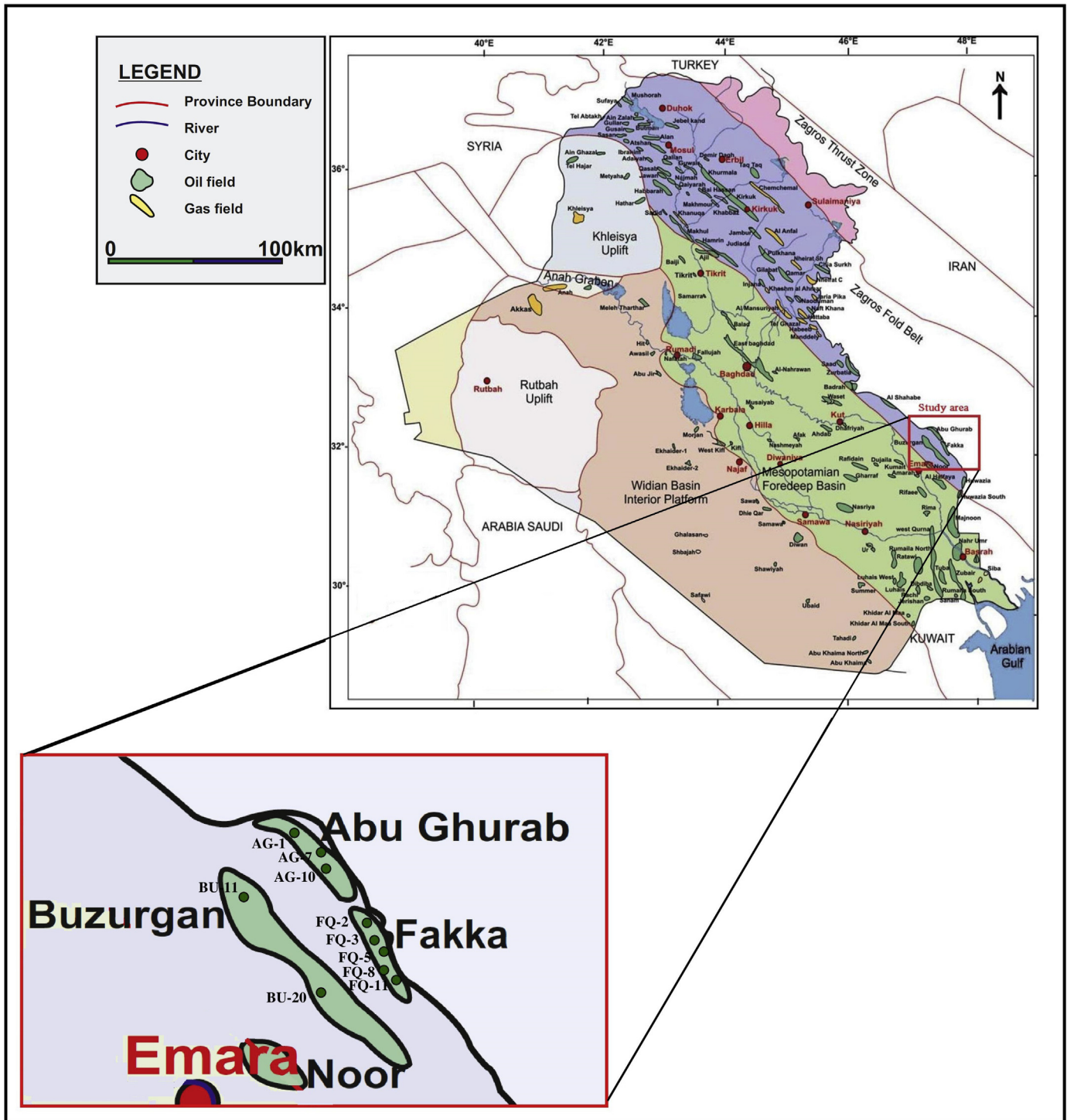
Fig. 1. Location map for the northeast Arabian Peninsula in Iraq, which shows Zagros Fold Belt with oil and gas field locations, including study oilfield locations (modified after Al-Ameri and Zumberge, 2012).

samples from different Cretaceous and Tertiary petroleum reservoirs in the Fakka, Buzurgan and Abo Gharab oilfields from the southern Zagros region (Table 1) were characterized by a variety of biomarker and non-biomarker data. The main objectives of the current study were to: (1) characterize the oil types and compositions; (2) characterize the source organic matter input, depositional conditions, and thermal maturity, and (3) establish tentative correlation between source rock and oil. This study also aims to

provide further insight into the basin's source rock potential for future petroleum exploration.

2. Geological setting

Zagros Fold Belt extends throughout the elongated folded zone area between the thrust zone in the triple junction boundary with Iran and Turkey (Fig. 1a). The Zagros Fold Belt is located in the

Table 1
Bulk property and chemical composition results of the crude oils from three oilfields (i.e., Fakka, Abo Ghurab and Buzergan) in the southern Zagros Fold Belt, Iraq.

Oilfields	Wells	Samples ID	Reservoir/age	Depth (ft)	API	S (%)	V ppm	Ni ppm	V/Ni	V/(V + Ni)	Fractions (wt%)			
											Sat.	Aro.	Res.	Asp.
Fakka field	FQ-2 well	IQ0143	Jeribe/Miocene	9974	20.1	3.90	73	25	2.92	0.74	22.5	52.7	12.3	12.5
	FQ-8 well	IQ0145	L. Kirkuk Group/Lower Oligocene	11,056	21.5	3.89	53	18	2.94	0.75	24.4	51.6	13.5	10.5
		IQ0146	L. Kirkuk Group/Lower Oligocene	12,762	19.5	3.85	62	22	2.82	0.74	20.6	53.3	15.6	10.5
	FQ-5 well	IQ0148	Mishrif/Cenomanian/Turonian	13,123	22.7	4.19	83	25	3.32	0.77	23.9	48.2	15.2	12.7
	FQ-3 well	IQ0151	Mishrif/Cenomanian/Turonian	12,664	20.6	3.67	84	29	2.90	0.74	26.2	42.1	14.2	17.5
	FQ-11 well	IQ0156	U. Kirkuk Group/Miocene	10,335	17.4	4.01	60	32	1.88	0.65	19.6	49.2	18.2	13.1
Abo Ghurab field	AG-1 well	IQ0157	M. Kirkuk Group/Oligocene	9941	21.0	4.63	112	49	2.29	0.70	21.1	48.0	16.0	14.9
	AG-7 well	IQ0150	U. Kirkuk Group/Miocene	9675	22.4	4.24	98	39	2.51	0.72	23.1	48.2	15.5	13.2
	AG-10 well	IQ0147	Jeribe/Miocene	9652	19.8	4.11	101	40	2.53	0.72	23.4	49.0	14.7	12.9
Buzergan field	BU-20 well	IQ0144	U. Kirkuk Group/Miocene	10,007	18.9	2.56	19	7	2.71	0.73	21.3	41.2	14.9	22.6
	BU-11 well	IQ0155	Jeribe/Miocene	9236	25.7	5.12	126	35	3.60	0.78	24.0	49.6	13.2	13.2

S—Sulphur, V—Vanadium, Ni—Nickel, Sat.—Saturated hydrocarbons, Aro.—Aromatic hydrocarbons, Res.— Resin, Asp.—Asphaltene.

north-eastern Arabian Plate and formed during the closing of the Tethys paleo-ocean, which includes the NW-trending Zagros Fault system through a series of composite faults oriented between N120° and N125° (Aqrawi et al., 2010). These faults were reactivated with normal displacement in the Maastrichtian to form half grabens accompanied by Shiranish sediment accumulation (Kent, 2010). The anticlines are fault-propagation folds developed by the most recent tectonic events in the long history of the underlying faults, which existed prior to the Zagros Orogeny (Kent, 2010). This structural framework of the Zagros Fold Belt produced the largest hydrocarbon accumulations in north Iraq oil and gas fields (Fig. 1).

The sedimentary rocks in the Zagros Fold Belt study area range in age from Jurassic to Tertiary, which is dominated by a thick Mesozoic succession (Fig. 2). The sedimentary rocks are composed of marine and subordinate lagoonal sediments (Buday, 1980) made up of carbonate, shale and anhydrite (Fig. 2). The Early Jurassic Adayah, Mus and Alan formations are primarily composed of bedded anhydrite with subordinate pseudo-oolitic limestone and indeterminate gastropod debris, which are considered as the seal rocks for reservoir hydrocarbons in south Iraq. The Middle Jurassic Sargelu Formation overlays conformably the Alan Anhydrite Formation (Fig. 2). The Sargelu Formation extends through the northern and southern basin. It is composed of bituminous limestone, dolomitic limestone and black shales with streaks of thin black chert in the upper portion with primarily *Posidonia* spp., *Parkinsonia* sp., *Stephanoceras* sp. and *Rhynchonella* spp. fossils, plant fragments, and poor ammonite impressions (van Bellen et al., 1959). The Sargelu Formation is overlain by the bituminous limestone and marl of the Late Jurassic Naokelekan Formation (Fig. 2). In the study region, the Naokelekan Formation is overlain by the Barsarin Formation, composed of limestones and evaporite layers (van Bellen et al., 1959). The Barsarin Formation is a lateral equivalent of the well known Gotnia Anhydrite Formation, which is an important regional seal for hydrocarbons and extends through the Mesopotamian Basin and the Zagros Fold Belt to a limited extent (Al-Ameri and Zumberge, 2012). The Gotnia Anhydrite Formation diminishes northward and is replaced by the Barsarin Formation in the Zagros Fold Belt. The first appearance of brown to dark shales or argillaceous limestones above the stromatolitic limestone beds of the Barsarin Fm. is defined as the base of the Chia Gara Formation (Mohialdeen, 2007). The contact is sharp and abrupt and considered as conformable (Buday, 1980). The Chia Gara Formation consists of organic-rich limestones and calcareous shales (marls) (Fig. 2), with rich ammonite faunas and diverse foraminifera, radiolarian, ostracodes and tintinnid species (Mohialdeen, 2007). The calpionellid fossils, especially *Calpionella alpine* Lorenz, and *Crassicollaria parvula* Remane (Mohialdeen, 2007), indicate a Late Tithonian to Berriasian age (Haq, 1980). The lithofacies of the Chia

Gara sediments reflect a reducing marine environment (Buday, 1980; Jassim and Goff, 2006; Mohialdeen et al., 2013).

The Cretaceous units comprise the Sarmord, Qamchuqa, Dokan, Gulneri, Kometan, Shiranish, and Tanjero formations deposited during Early to Late Cretaceous time (Fig. 2). These sedimentary rocks are composed of mainly marine carbonates and subordinate clastics sediments (Fig. 2). The Cretaceous rocks in the basin are considered as potential source and reservoir rocks (Dunington, 1958; Al-Ameri and Zumberge, 2012). The Cretaceous formations are overlain by a thick Tertiary succession, which includes Aliji, Jaddala, Serikagni, Dhiban, Jeribe and Fars formations (Fig. 2). Lower Tertiary rocks in the basin are also considered as gas and oil reservoir rocks (Dunington, 1958; Al-Ameri and Zumberge, 2012) and comprise fractured and vuggy carbonate rocks (Fig. 2). The Middle Miocene Fatha (Lower Fars) member is an excellent seal for the underlying Cretaceous and lower Tertiary reservoirs, and it primarily includes bedded anhydrite with shale intercalation (Fig. 2). The Fatha Anhydrite seal disappears in north and northeast Iraq (Al-Juboury and McCann, 2008). The Pliocene Muqdadia deposits cover the Miocene rocks (Fig. 2), which are composed of conglomerates (Fig. 2).

3. Samples and experimental methods

In this study, eleven crude oil samples from different Cretaceous and Tertiary petroleum reservoirs in the oilfields of the southern Zagros Fold Belt were selected for geochemical analyses (Fig. 1; Table 1). The geochemical analyses performed include API gravity, sulphur, and trace element (Ni, V) determination, bulk carbon isotope composition, asphaltene content, gas chromatography (GC) and gas chromatography—mass spectrometry (GC—MS). The crude oil samples were provided from the South Oil Company in Iraq and the geochemical analyses were carried out at GeoMark Research. Houston, Texas.

API gravity was measured on the crude oil samples according to Hunt (1996). About 1—2 ml of whole oil was injected using a syringe into an Anton Par DMA 500 density meter. This process is triplicated for each oil in order to validate accuracy and reproducibility. The whole oil samples were analysed by a vario ISOTOPE select elemental analyzer instrument to provide measurements of total sulphur (S) content. The whole crude oil samples were treated to precipitate asphaltenes by adding *n*-pentane. The asphaltene precipitate was left for 5 min and then allowed to settle in a refrigerator for at least 1 h. The precipitated asphaltenes were then filtered. The maltene fractions of the oils were adsorbed onto silica gel topped with alumina oxide and then fractionated into saturated hydrocarbons, aromatic hydrocarbons and polar compounds using liquid column chromatography. Elution with *n*-pentane produced
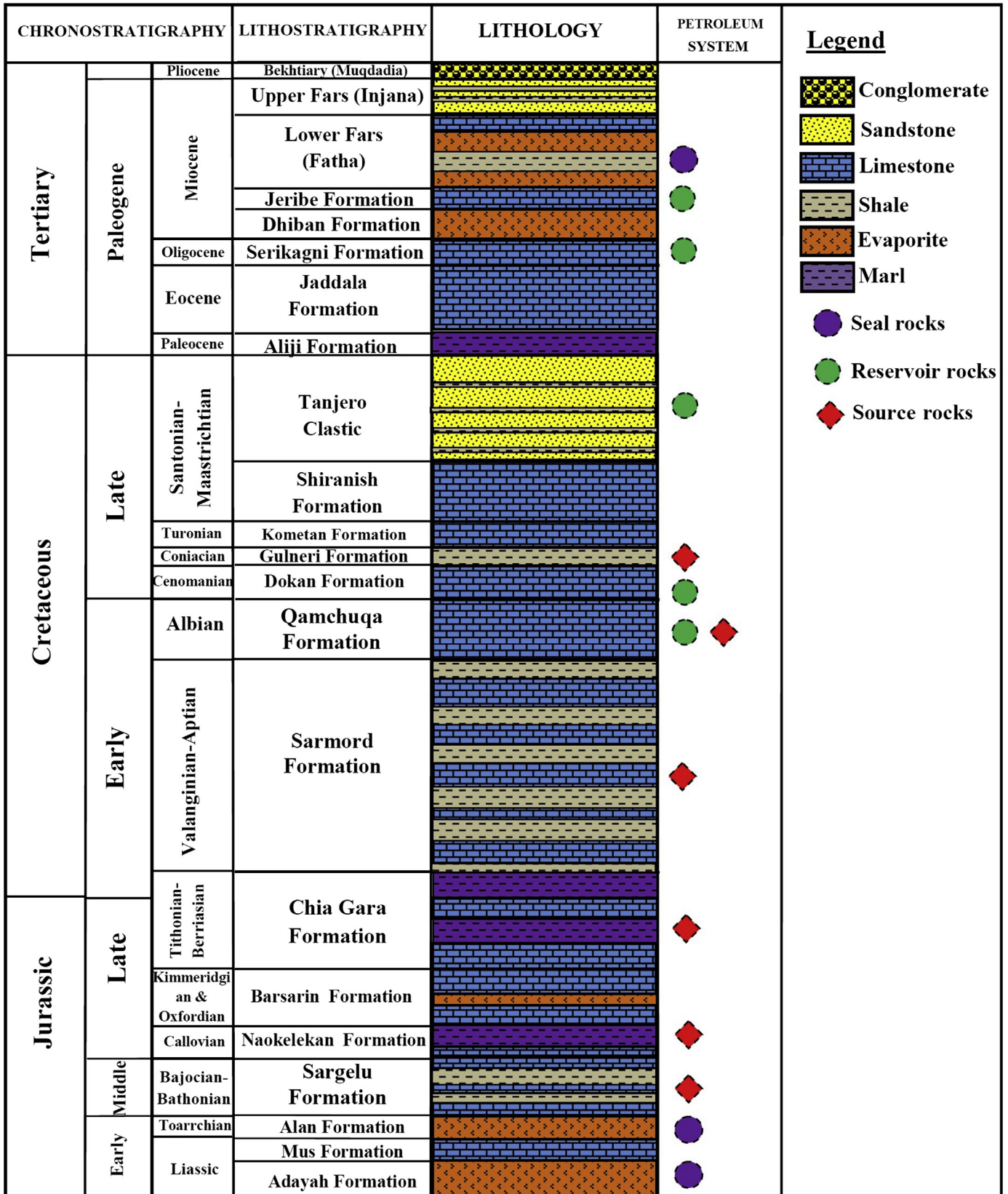
CHRONOSTRATIGRAPHY			LITHOSTRATIGRAPHY	LITHOLOGY	PETROLEUM SYSTEM
Tertiary	Paleogene	Pliocene	Bekhtiary (Muqdadia)		
		Miocene	Upper Fars (Injana)		
			Lower Fars (Fatha)		Seal
			Jeribe Formation		Reservoir
			Dhiban Formation		
		Oligocene	Serikagni Formation		Reservoir
		Eocene	Jaddala Formation		
		Paleocene	Aliji Formation		
Cretaceous	Late	Santonian-Maastrichtian	Tanjero Clastic		Reservoir
			Shiranish Formation		
		Turonian	Kometan Formation		
		Coniacian	Gulneri Formation		Source
		Cenomanian	Dokan Formation		Reservoir
	Early	Albian	Qamchuqa Formation		Reservoir / Source
		Valanginian–Aptian	Sarmord Formation		Source
Jurassic	Late	Tithonian–Berriasian	Chia Gara Formation		Source
		Kimmeridgian & Oxfordian	Barsarin Formation		
		Callovian	Naokelekan Formation		Source
	Middle	Bajocian–Bathonian	Sargelu Formation		Source
	Early	Toarrchian	Alan Formation		Seal
		Liassic	Mus Formation		
			Adayah Formation		Seal

Legend

- Conglomerate
- Sandstone
- Limestone
- Shale
- Evaporite
- Marl
- Seal rocks
- Reservoir rocks
- Source rocks

Fig. 2. Lithostratigraphic section for the Zagros Fold Belt in northeast Iraq (modified after Al-Ameri and Zumberge, 2012).

the saturated hydrocarbon fraction, elution with a dichloromethane (DCM) produced the aromatic hydrocarbon fraction, and elution with a methanol (CH₃OH) produced the polar compounds.

The saturated fraction was analysed using GC and GC-MS instruments. The GC analysis was performed using a Hewlett-Packard 5890GC equipped with a 30 × 0.32 mm i.d. DB-1 fused silica capillary column. The temperature was programmed from 20 to 310 °C at a rate of 4 °C/min, and then held for 32 min at 310 °C. The GC−MS analysis was carried out using a Finnigan TSQ-70 mass spectrometer with a gas chromatograph attached directly to the ion source (70 eV ionization voltage, 200 milliamps filament emission current, 230 °C interface temperature) in full scan (50−550 amu)
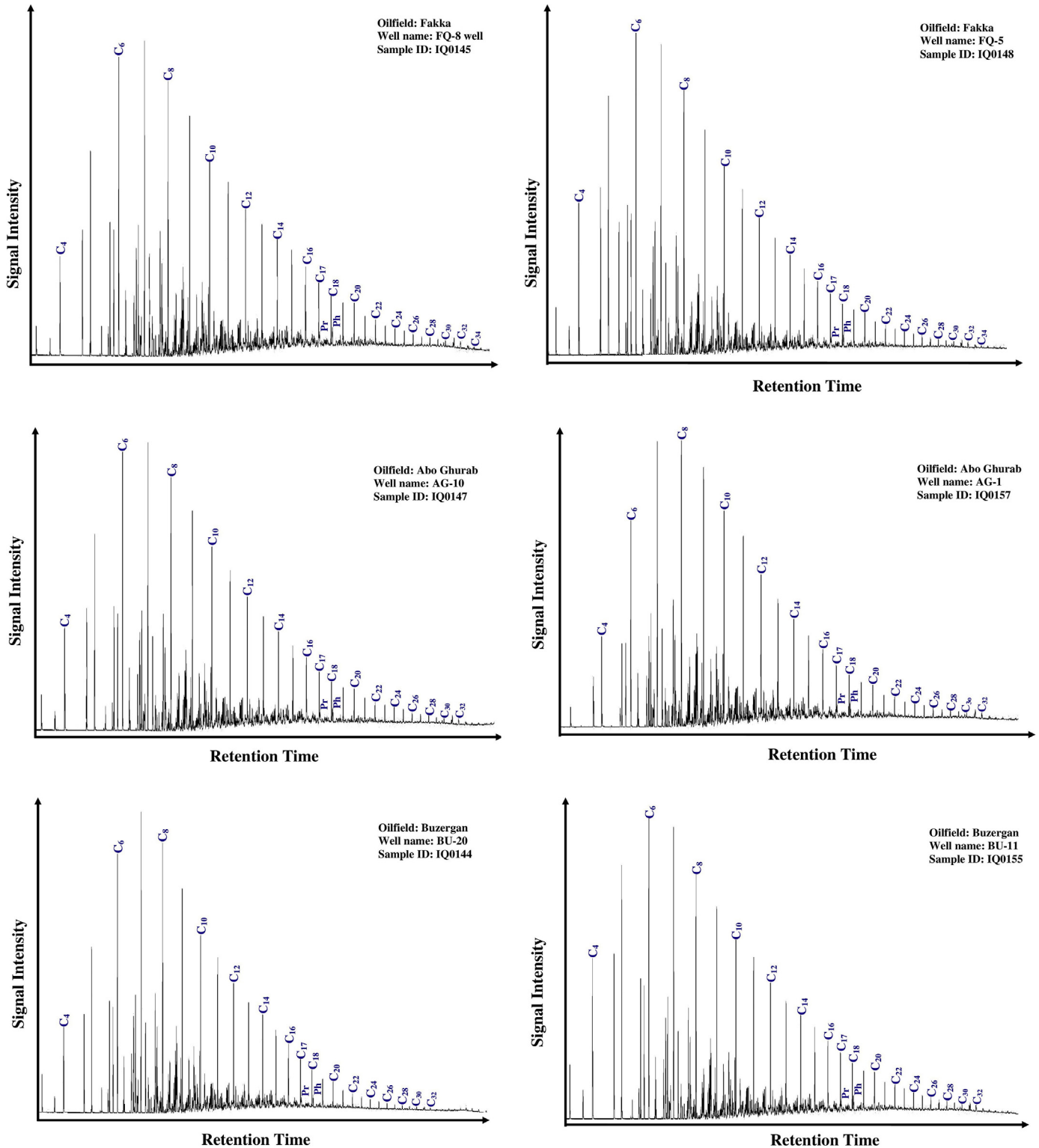
Fig. 3. Gas chromatograms of saturated hydrocarbon fraction of six representative analysed oil samples.

mode. The GC-MS temperature conditions were programmed from 40 °C for 1.5 min to 310 °C at a rate of 4 °C/min, and then held for 31 min at 310 °C. The selected ion monitoring capabilities of the data acquisition system permitted specific ions to be monitored, such as terpanes (m/z 191), and steranes (m/z 217) of saturated hydrocarbon fractions. Biomarker ratios as presented by previous workers (e.g. Philp, 1985; Peters et al., 2005; Hakimi et al., 2011) were calculated using measured peak heights from mass fragmentograms.

Saturated and aromatic fractions were also analysed for their stable carbon isotopic compositions ($\delta^{13}C$) using an Isoprime vario ISOTOPE select elemental analyzer and VisION isotope ratio mass spectrometer (IRMS). Carbon isotope data are reported using standard delta-notation relative to Pee Dee belemnite (PDB).

4. Results and discussion

4.1. Bulk oil characteristics

The bulk characteristics of the analysed oils are presented in Table 1, which include oil properties and compositions.

The oil samples from oilfields in the southern Zagros Fold Belt Basin have relatively low API gravity values in the range of 17.4—22.7° (Table 1). Such lower API gravity values are generally associated with either biodegraded oils or sulphur-rich oils (Baskin and Peters, 1992). Based on the character of the gas chromatograms (Fig. 3), there is no biodegradation observed in the oil samples. This is consistent with complete suite of acyclic isoprenoids (e.g. pristane and phytane) and low molecular-weight *n*-alkanes (Baskin and Peters, 1992; Larter et al., 2005). Low concentrations of asphaltenes compared to hydrocarbon fractions (saturated and aromatic hydrocarbons) (Table 1), further suggest the oil samples were not biodegraded, because high asphaltene contents are signs of a biodegradation process (Peters et al., 2005). Therefore, the absence of biodegradation suggests that the low API gravity values in the analysed oil samples are associated with sulphur-rich

kerogens. This finding is supported by high concentrations of total sulphur (S) content in the analysed oil samples (Table 1).

The sulphur content reflects the type of organic input and its depositional environment (Gransch and Posthuma, 1974; Moldowan et al., 1985). Carbonate source rocks deposited in a marine environment under sulphate-reducing conditions generally have high sulphur contents, whereas source rocks deposited in siliciclastic environment usually have low sulphur contents (Gransch and Posthuma, 1974). In this study, the analysed oils have high sulphur contents, ranging from 2.56 to 5.12 wt%, suggesting that the oils were generated from carbonate source rocks (Gransch and Posthuma, 1974; Huang and Pearson, 1999). This also suggests that the analysed oils were possibility generated from source rocks containing type II-S kerogen.

4.2. Nickel and vanadium

Crude oils contain metals; particularly nickel (Ni) and vanadium (V), in variable amounts. Ni and V are usually associated with the heavy, polar NSO fraction of crude oils and, as such, should increase in concentration with evaporation and biodegradation (Lewan, 1984). The concentrations of the V and Ni metals can provide insight into the depositional environment (Lewan, 1984; Barwise, 1990; Wenger et al., 2002). In general, oils generated from marine carbonate or siliciclastic source rocks contain moderate to high sulphur and variable amounts of Ni and V (Barwise, 1990), whereas land plant-derived oils contain low sulphur, and relatively low Ni and V metals (Wenger et al., 2002). In this study, the analysed oil samples have V and Ni values in the range of 19—126 ppm and 7—49 ppm, respectively (Table 1). These Ni and V contents together with high sulphur content (>2 wt %) suggests a marine carbonate source rock deposited under reducing conditions (Fig. 4). The higher ratios of V/Ni (Table 1) suggest that the oils were generated from a marine carbonate source rock deposited under reducing conditions, because V is usually enriched in comparison to Ni in anoxic (reducing) marine conditions (Barwise, 1990; Galarraga
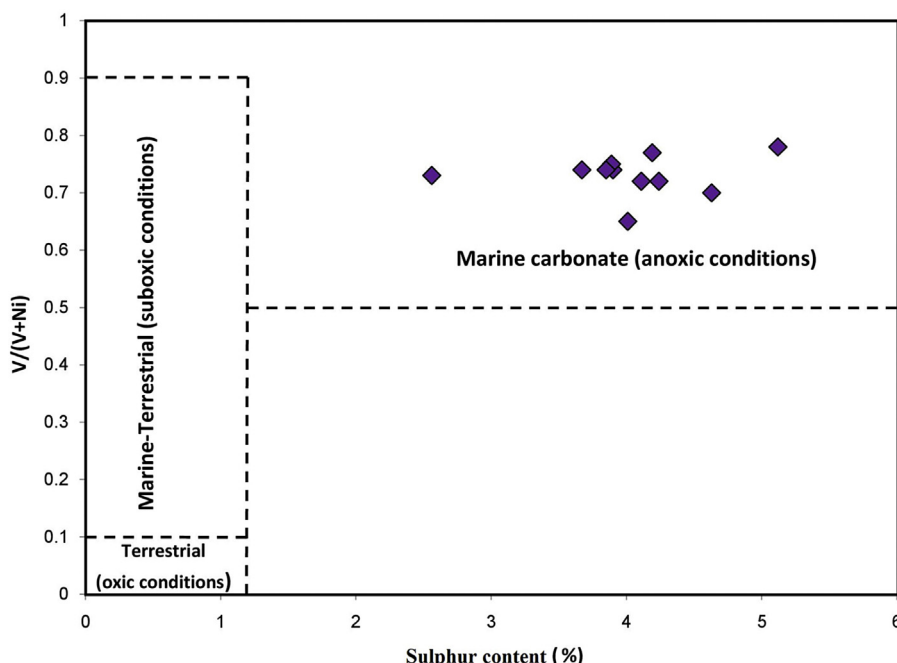

Fig. 4. Trace element ratios of V/(V + Ni) versus sulphur content (wt.%) of the analysed oil samples (modified after Galarraga et al., 2008).

Table 2
Bulk carbon isotope (‰) with selected biomarker parameters of the crude oil samples from southern Zagros Fold Belt, illustrating source organic matter, depositional environment conditions and thermal maturity.

Samples ID	n-alkane and isoprenoids				Triterpanes and terpanes (m/z191)								Steranes (m/z217)				Regular steranes (%)			Isotope compositions (‰)	
	Pr/Ph	Pr/C$_{17}$	Ph/C$_{18}$	CPI	C$_{32}$ 22S/(22S + 22R)	MC$_{30}$/C$_{30}$	C$_{29}$/C$_{30}$	Ts/Tm	G/C$_{30}$	C$_{35}$Ho/C$_{34}$Ho	HOI	HCR$_{31}$/HC$_{30}$	C$_{29}$ 20S/20S + 20R	C$_{29}$ ββ/(ββ+αα)	diasterane/ sterane	C$_{27}$/C$_{29}$ Regular steranes	C$_{27}$	C$_{28}$	C$_{29}$	Saturated	Aromatic
IQ0143	0.89	0.26	0.38	1.10	0.53	0.09	1.91	0.24	0.16	1.00	0.09	0.36	0.34	0.43	0.15	0.79	46.46	16.68	36.87	−27.51	−27.53
IQ0145	0.83	0.24	0.36	0.86	0.54	0.09	1.88	0.24	0.15	0.97	0.10	0.36	0.34	0.44	0.16	0.80	46.28	16.56	37.16	−27.52	−27.63
IQ0146	0.97	0.31	0.43	0.90	0.53	0.08	2.07	0.24	0.16	1.00	0.08	0.37	0.34	0.44	0.11	0.79	46.30	17.23	36.47	−27.46	−27.60
IQ0148	0.77	0.21	0.34	0.86	0.55	0.06	1.75	0.21	0.14	1.02	0.11	0.36	0.41	0.44	0.18	0.77	48.35	14.26	37.39	−27.62	−27.69
IQ0151	0.75	0.19	0.31	0.91	0.56	0.09	1.54	0.24	0.13	1.01	0.10	0.36	0.42	0.45	0.24	0.84	47.09	13.54	39.37	−27.81	−27.68
IQ0156	0.96	0.31	0.42	0.85	0.52	0.08	2.04	0.24	0.18	1.03	0.09	0.36	0.35	0.44	0.13	0.77	47.36	16.26	36.38	−27.36	−27.73
IQ0157	0.90	0.26	0.36	1.02	0.53	0.08	1.82	0.23	0.14	1.02	0.08	0.36	0.31	0.42	0.13	0.75	46.23	19.22	34.54	−27.72	−27.50
IQ0150	0.84	0.25	0.36	0.87	0.52	0.09	1.81	0.23	0.15	1.05	0.10	0.37	0.35	0.43	0.15	0.81	45.19	18.24	36.58	−27.64	−27.62
IQ0147	0.94	0.27	0.36	0.95	0.53	0.09	1.73	0.24	0.15	1.03	0.09	0.36	0.35	0.45	0.15	0.77	46.44	17.91	35.66	−27.52	−27.62
IQ0144	0.85	0.21	0.33	0.95	0.55	0.08	1.70	0.23	0.15	1.02	0.09	0.37	0.41	0.46	0.24	0.80	48.45	12.91	38.64	−27.68	−27.64
IQ0155	0.84	0.21	0.32	0.92	0.56	0.09	1.77	0.21	0.16	1.05	0.10	0.35	0.42	0.45	0.18	0.84	46.68	14.13	39.19	−27.67	−27.87

Pr–Pristane, Ts–(C$_{27}$ 18α(H)-22,29,30-trisnorneohopane), CPI–Carbon preference index (1): [2(C$_{23}$ + C$_{25}$ + C$_{27}$ + C$_{29}$)/(C$_{22}$ + 2[C$_{24}$ + C$_{26}$ + C$_{28}$] + C$_{30}$)], Ph–Phytane, Tm–(C$_{27}$ 17α(H)-22,29,30-trisnorhopane), HCR$_{31}$/HC$_{30}$: C$_{31}$ regular homopane/C$_{30}$ hopane, HOI: homopane index = C$_{35}$ (R + S)/total homopanes C$_{31}$- C$_{35}$ (R + S), C$_{30}$M/C$_{30}$H = C$_{30}$ moretane/C$_{30}$ hopane, C$_{29}$/C$_{30}$: C$_{29}$ norhopane/C$_{30}$ hopane, C$_{35}$Ho/C$_{34}$Ho = C$_{35}$ homopane/C$_{34}$homopanes, G/HC$_{30}$ = Gammacerane/C$_{30}$ hopane.

et al., 2008).

4.3. Carbon isotope ratio values

The carbon isotope ratio values of oils have been used to evaluate the source of organic matter and depositional environments of their source rocks and to determine the genetic relationship between oils and their potential source rocks (e.g., Summons et al., 1992; Boreham et al., 2001). Organic carbon isotope analysis is widely used to classify the environments of oils and source rock as marine or non-marine (terrigenous) by plotting the bulk values of the δ^{13}C saturated fractions versus those of their aromatic fractions (Sofer, 1984; Collister and Wavrek, 1996). The analysed oil samples have δ^{13}C values of their saturated and aromatic hydrocarbon fractions ranging from −27.36‰ to −27.81‰ and −27.50‰ to −27.87‰, respectively (Table 2), implying marine origin (Fig. 5).

4.4. Biomarker distributions

Biomarker distributions are commonly used to describe source input of organic matter and paleodepositional conditions (Waples and Machihara, 1991; Hunt, 1996; Peters et al., 2005). In this study, the biomarker distributions of n-alkanes, isoprenoids, hopanes and steranes were performed on saturated hydrocarbons. Peak assignments are listed in Appendix 1 and the calculated ratios are shown in Table 2.

Normal alkanes and isoprenoids are present and typically represent the dominant compounds, which show the presence of a full suite of saturated hydrocarbons between C$_4$–C$_{32}$ n-alkanes (Fig. 3). The n-alkanes display a clear dominance of short-chain n-alkanes (C$_4$-C$_{20}$) relative to long chain n-alkanes (C$_{24}$-C$_{32}$) with a maximum at C$_6$-C$_9$ (Fig. 3). This n-alkane distribution suggests a high contribution of aquatic organic matter input (e.g., Cranwell, 1977; Brassell et al., 1978; Tissot and Welte, 1984). The carbon preference indices (CPI) are also calculated (Table 2). The relatively low carbon preference index values (CPI < 1) are obtained from the analysed oil samples. The CPI is influenced by thermal maturity and decreases with increasing thermal maturity (Bray and Evans, 1961).

Acyclic isoprenoids occur in all of the analysed oil samples (Fig. 3), with pristane (Pr) and phytane (Ph) usually the most dominant acyclic isoprenoids hydrocarbons in terms of concentration (Powell and McKirdy, 1973). The analysed oils have an obvious domination of phytane (Ph) relative to pristane (Pr) (Fig. 3), thus giving distinctively low Pr/Ph ratios of 0.75−0.97, suggesting source rock deposition under reducing conditions (Didyk et al., 1978; Chandra et al., 1994; Peters et al., 2005). Furthermore, lower pristane/n−C$_{17}$ and phytane/n−C$_{18}$ ratios (Table 2), suggest marine algal organic matter preserved under reducing conditions (Fig. 6).

Terpane and sterane biomarkers were also used to confirm the origin of organic matter input and depositional environment.

The m/z 191 mass fragmentograms of the saturated hydrocarbon fractions of all the oil samples show high proportions of hopanes relative to tricyclic terpanes (Fig. 7). The hopane biomarkers are dominated by C$_{30}$-hopane and C$_{29}$-norhopane, with significant presence of 18α (H)-trisnorhopane (Ts), and a considerable quantity of homohopanes (C$_{31}$−C$_{35}$) (Fig. 7). The C$_{29}$-norhopane is higher than hopane in all of the analysed oil samples (Fig. 8), with C$_{29}$/C$_{30}$ ratios greater than 1 (Table 2). The predominance of C$_{29}$-norhopane is consistent with a carbonate source rock (e.g. Clark and Philp, 1989).

The homohopane distributions are dominated by C$_{31}$ homohopane (Fig. 7). The homohopanes index [C$_{35}$/(C$_{31}$−C$_{35}$)] can be used to evaluate redox conditions during deposition of the source rock (Peters et al., 2005). The analysed oils have relatively high
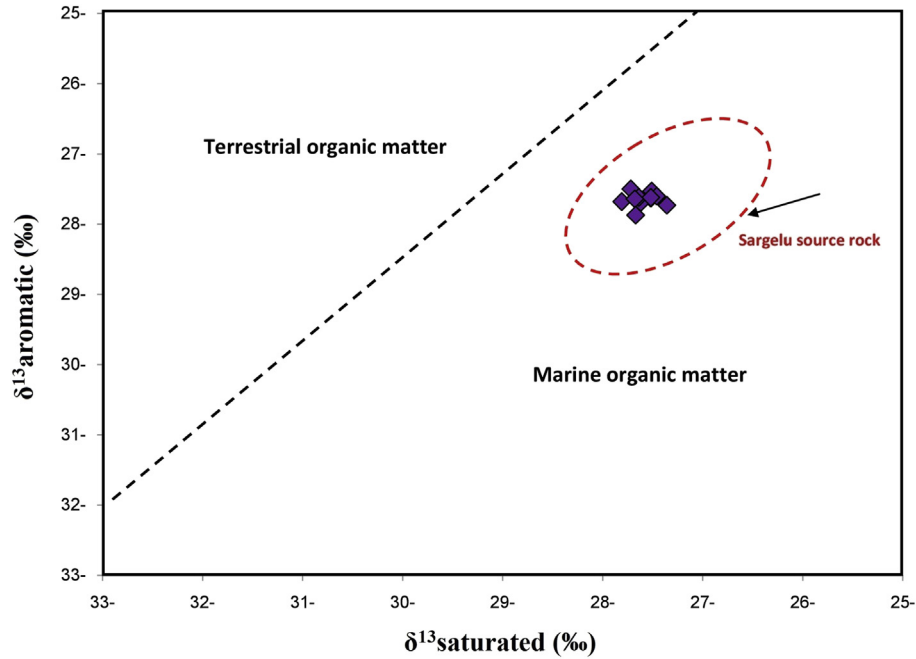
Fig. 5. Plot of the δ¹³C values of aromatic fractions versus of the δ¹³C values of saturated fractions for analysed oils samples and zone of the Middle Jurassic Sargelu source rock in the northern basin (after Al-Ameri et al., 2013; Sachsenhofer et al., 2015). The line represents the best fit separation for waxy and non-waxy oils and is described by the equation δ¹³C Aromatic = 1.14 δ¹³C saturated +5.46 (after Sofer, 1984).

homohopane indices [$C_{35}/(C_{31}-C_{35})$] (Table 2), suggesting anoxic conditions (Mohialdeen et al., 2013). This is consistent with the relatively high homohopane C_{35} concentrations compared to C_{34} homohopane (Fig. 7), with C_{35}/C_{34} ratios in the range of 0.97–1.05 (Table 2).

The C_{31}-22R-hopane/C_{30}-hopane ratios have been calculated and used to distinguish between different depositional environments (Peters et al., 2005). C_{31}-22R-hopane/C_{30}-hopane ratios higher than 0.25 indicate a marine environment, whereas lower ratios (<0.25) have been found in oils derived from lacustrine and deltaic source rocks (Peters et al., 2005). The C_{31}-22R-hopane/C30-hopane ratios (>0.30) confirm that the analysed oils were derived from a marine carbonate source rock (Fig. 8). In addition, gammacerane is also recognized in all of the analysed oil samples
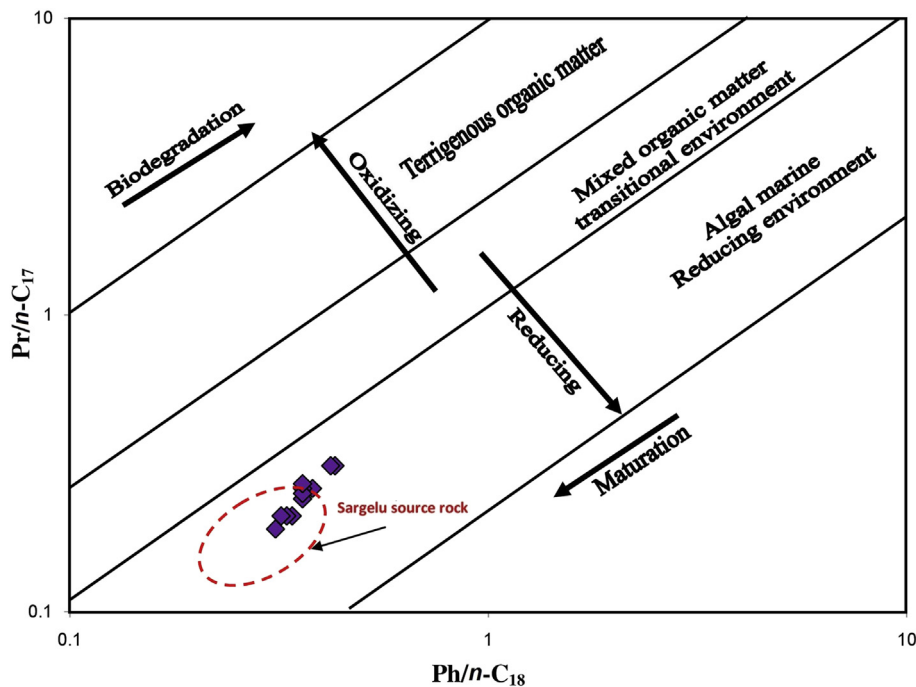
Fig. 6. Pr/n-C_{17} ratio versus Ph/n-C_{18} ratios of the analysed oil samples and zone of the Middle Jurassic Sargelu source rock in the northern basin (after Al-Ameri et al., 2013; Sachsenhofer et al., 2015), showing marine reducing conditions.
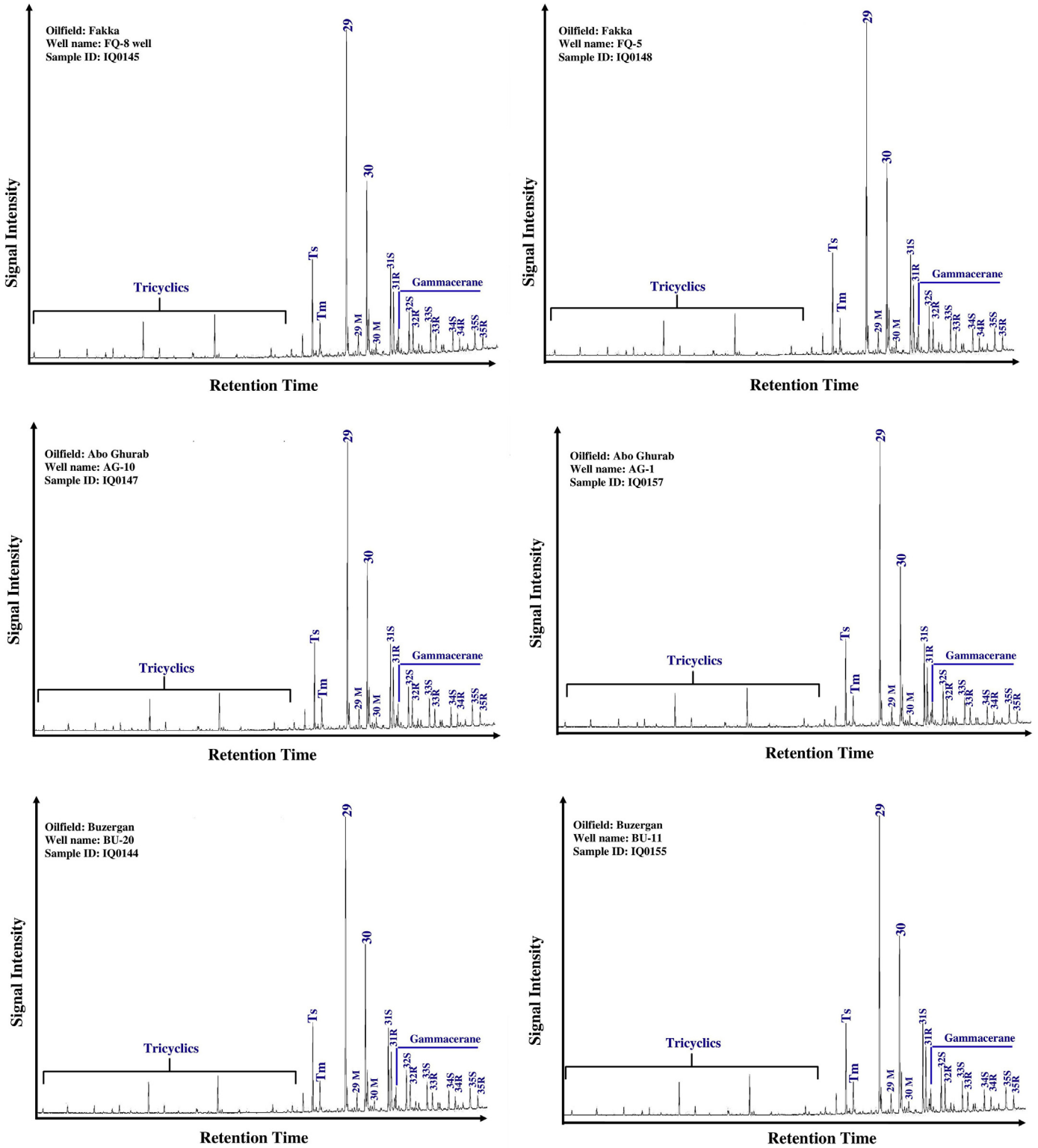
Fig. 7. Terpanes distribution in the *m/z* 191 mass fragmentograms in the saturated fraction of six representative oil samples.

(Fig. 7). Gammacerane is a strong indicator of hypersalinity and/or water column stratification conditions during deposition of the source rock (Moldowan et al., 1985; ten Haven et al., 1989; Sinninghe Damsté et al., 1995). In this study, the presence of gammacerane with a low gammacerane index (G/C_{30}) of the analysed oils (Table 2) is regarded as an indicator of high salinity stratification and a possible marker for photic zone anoxia during source rock deposition. The high salinity stratification conditions during deposition of source rock are supported by the high sulphur content of the analysed oils (Table 1). Moreover, the absence of 18a (H)-oleanane biomarker in all analysed oil samples (Fig. 7) suggest a high contribution of aquatic organic matter (i.e., plankton/algal and microorganisms). Oleanane is a strong indicator of terrestrial angiosperm plant input in rocks of Late Cretaceous or younger age (Ekweozor and Telnaes, 1990). The sterane and diasterane biomarkers can also be recognized in the analysed oil samples (Fig. 9). The m/z 217 mass fragmentograms of all the analysed oil samples are dominated by steranes over diasteranes, with high concentrations of C_{27} regular steranes (Fig. 9). The diasterane/regular sterane ratio of the analysed oils is also calculated and shows low values in the range of 0.11−0.24 (Table 2). This can also be indicative of a carbonate source rock (Peters and Fowler, 2002). Relative abundances of C_{27}, C_{28} and C_{29} regular steranes were calculated and the results show that the analysed oils have a high proportion of C_{27} (45.19−48.45%) compared to C_{28} (12.91−19.22%) and C_{29} (34.54−39.37%) regular steranes (Table 2). The regular sterane distributions as shown in Fig. 10 suggest a predominantly planktonic/algal source input. This is also demonstrated by low values of C_{29}/C_{27} regular steranes ratio (Fig. 11) (Markovaa et al., 2016). The regular sterane ratio ternary diagram also suggests one genetic family (Fig. 10).

4.5. Maturity of oils

The maturity of the analysed oil samples from southern Zagros Fold Belt was primary evaluated using biomarker ratios such as

CPI, C_{32} hopanes 22S/(22S + 22R), Ts/Tm, moretane/hopane, C_{29} sterane 20S/(20S + 20R) and ββ/(ββ+αα) ratios (Table 2). The distribution of n-alkanes of the analysed oils (Fig. 3) exhibit relatively low CPI values, close to unity (Table 2), suggesting that the studied oils are mature (Bray and Evans, 1961). The ratios of 22S/(22S + 22R) for C_{32} hopanes are between 0.52 and 0.56, suggesting that they have reached the oil window and the oils are at least early mature (Seifert and Moldowan, 1986). This level of oil maturity is also supported by the C_{29} sterane 20S/(20S + 20R) and ββ/(ββ+αα) maturity ratios (Seifert and Moldowan, 1978, 1981). The analysed oils have relatively low C_{29} sterane 20S/ (20S + 20R) and ββ/(ββ+αα) ratios in the range of 0.31−0.42, 0.42−0.46, generally either at or close to thermal equilibrium, consistent with their generation from early-mature source rocks (Fig. 12).

The ratio of the 18a(H)-trisnorneohopane (Ts) and 17a(H)-trisnorhopane (Tm) biomarkers in the term Ts/Tm ratio is also used as a maturity indicator (Peters et al., 2005; Roushdy et al., 2010; El Nady et al., 2014), where Ts is more stable to thermal maturation than Tm. Thus, the Ts/Tm ratios increase with increasing maturity (Roushdy et al., 2010; El Nady et al., 2014). The relatively low Ts/Tm ratios of the analysed oils (0.21 and 0.24) are consistent with an early-mature source rock. The moretane/ hopane ratio further indicates the maturity of the source rocks and oils (Mackenzie et al., 1980; Seifert and Moldowan, 1986). The ratios of the moretane/hopane less than 0.10 indicate a mature source rock, whereas values of 0.80 indicate immature source rocks (Mackenzie et al., 1980). The values of the moretane/hopane with Ts/Tm ratio of the analysed oils reflect the same interpretation of an early-mature source rock (Fig. 13). This interpretation is confirmed by the relationship between isoprenoids Pr/n-C_{17} and Ph/n-C_{18} ratios (Fig. 6).

Non-biomarker parameters (i.e., API gravity and sulphur contents) have also been used to evaluate the level of thermal maturity of the oils that are not biodegraded (El-Gayar et al., 2002). The API gravity and sulphur content vary strongly with the maturity of oils
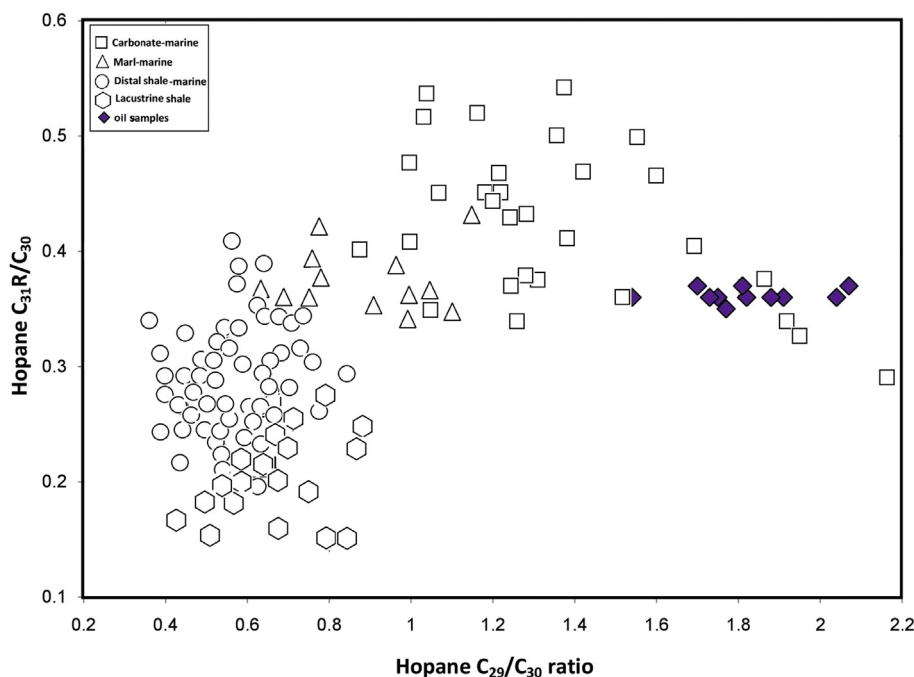

Fig. 8. Average hopane ratios of analysed oils from southern Iraq suggesting a carbonate source rock (SR). Other data points represent average oil values from 150 global petroleum systems from marine carbonate, distal marine shale, marine marl, and lacustrine shale source rocks (data from Peters et al., 2005).

(Barwise, 1990; El-Gayar et al., 2002). The sulphur content in crude oil decreases with increasing maturity, whereas the API gravity values increase (Barwise, 1990; El-Gayar et al., 2002). In this study, the oils are not biodegraded, therefore, API gravity and sulphur contents can be used as maturity indicators (Barwise, 1990; El-Gayar et al., 2002). The analysed oils have high sulphur contents

and relatively low API gravity values (Table 1). This is further evidence suggesting that the analysed oil samples were generated from early mature source rocks. This appears to result from the type of kerogen of the source rock, characterized by a high-S kerogen (Type II-S) (Baskin and Peters, 1992).
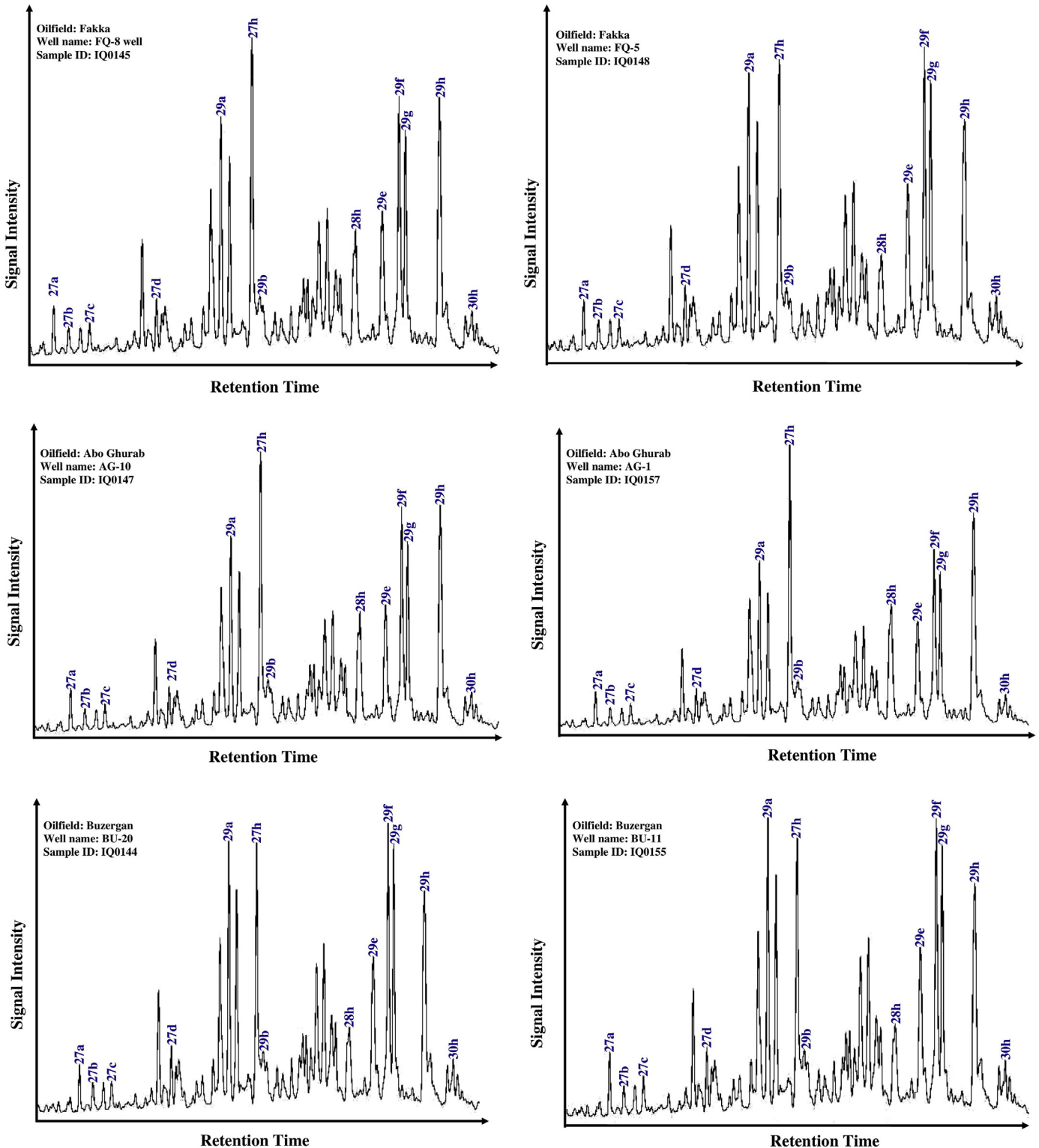
Fig. 9. Steranes and diasteranes distribution in the *m/z* 217 mass fragmentograms in the saturated fraction of six representative oil samples.
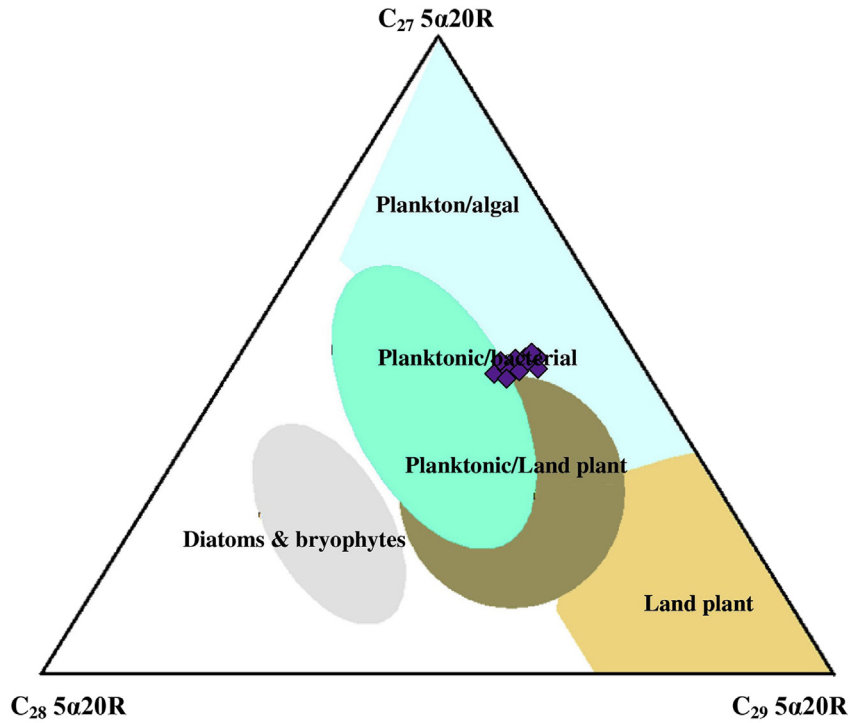
Fig. 10. Ternary diagram of regular steranes (C$_{27}$-C$_{29}$) indicating the relationship between sterane compositions in relation to organic matter input and depositional environments (modified after Huang and Meinschein, 1979).

4.6. Oil-source rock correlation

The results of this study indicate that the analysed oils in the southern Zagros Fold Belt were generated from a carbonate source rock bearing Type II-S kerogen dominated by algal organic matter, deposited in a marine environment under sulphate-reducing conditions. The genetic link between the analysed oils and their potential source rocks in the basin was investigated using previously published data on the Middle Jurassic Sargelu source rock from the Zagros Fold Belt (Al-Ameri et al., 2013; Sachsenhofer et al., 2015). The Sargelu Formation is exposed in the Zagros Fold Belt and extends from north to south of the Zagros Fold Belt (Al-Ahmed,
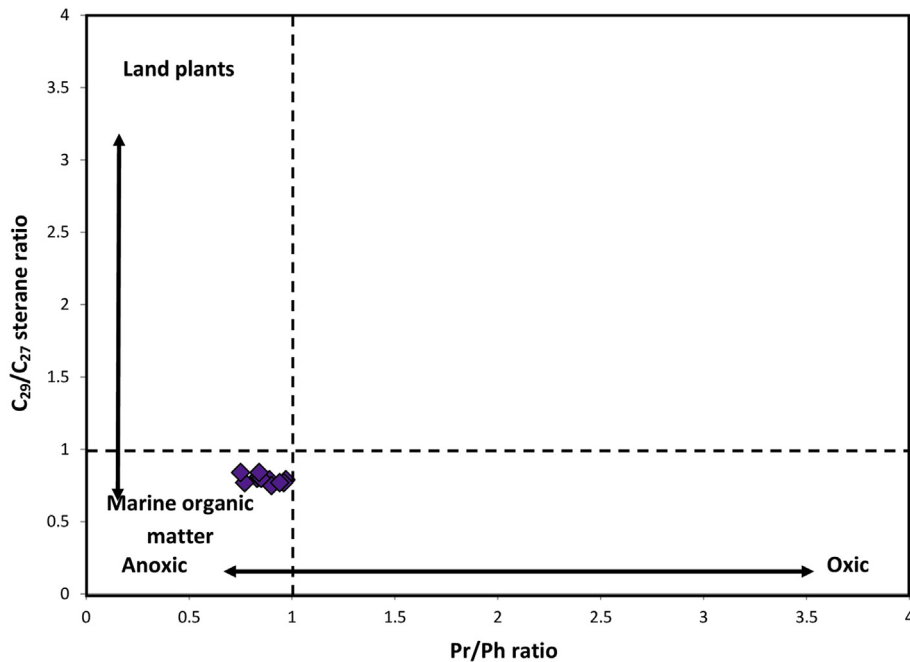
Fig. 11. Cross-plots for pristane/phytane versus C$_{29}$/C$_{27}$ regular steranes ratio, which provides an inference for a source rock deposited environment and lithology (modified after Peters et al., 2005).
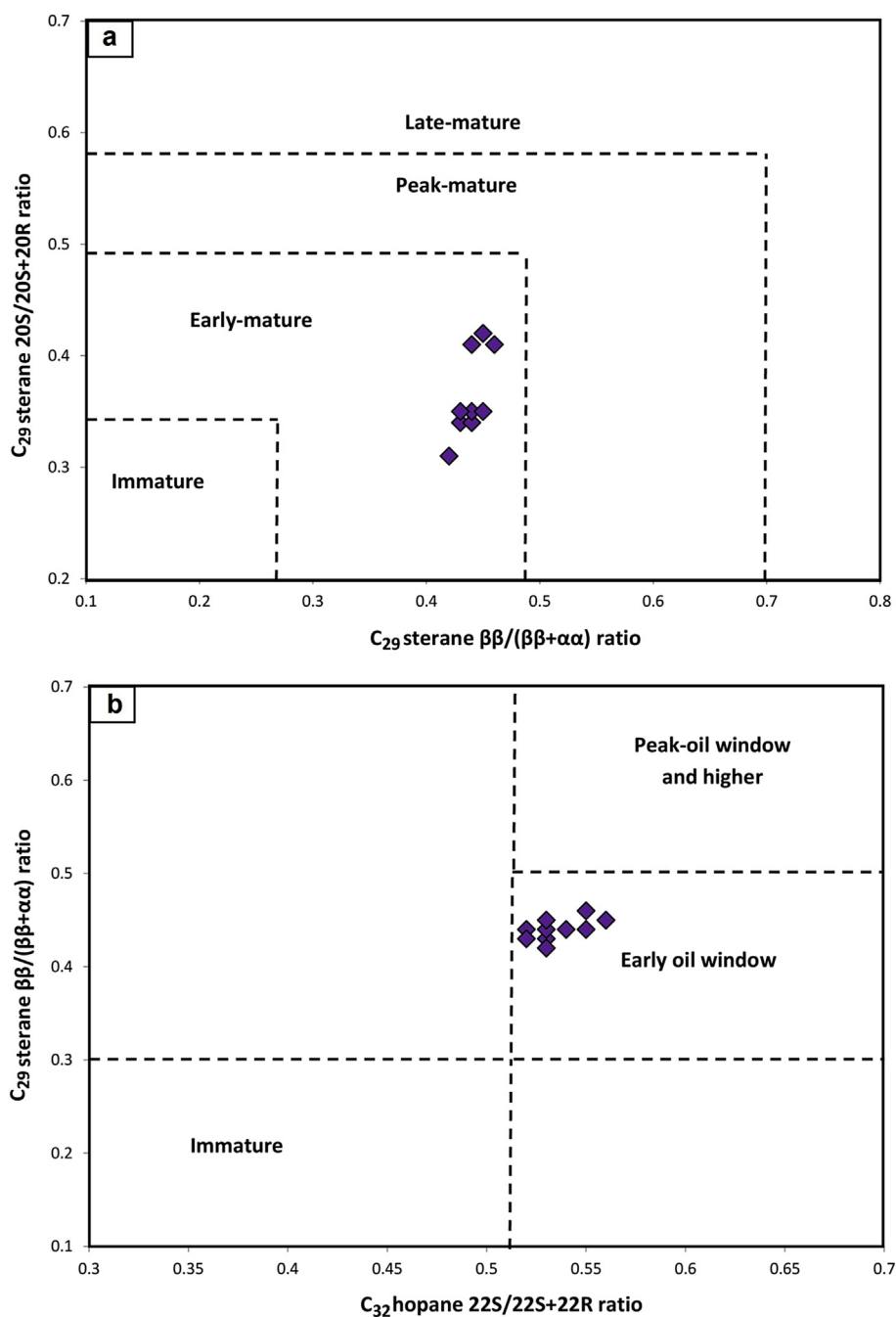
Fig. 12. A range of thermal maturity based on biomarker maturity parameters (a) C$_{29}$ sterane 20S/(20S + 20R) Vs. ββ/(ββ+αα) and (b) C$_{32}$ hopane 22S/(22S + 22R) versus C$_{29}$ sterane ββ/(ββ+αα) as modified after Peters et al. (2005).

2006; Al-Ameri et al., 2013; Sachsenhofer et al., 2015).

There are lines of evidence for a genetic link between the analysed oils and the Middle Jurassic Sargelu source rock.

The Middle Jurassic Sargelu source rock are bituminous limestones and black calcareous shales, with high TOC and sulphur contents and hydrogen index (HI) more that 400 mg HC/g TOC) (Sachsenhofer et al., 2015). Thus, this source rock contain type II-S kerogen and can generate early-mature sulphur-rich oils (Baskin and Peters, 1992). The biomarkers and bulk carbon isotope data of saturated and aromatic fractions for the Middle Jurassic Sargelu source rock suggest that this source rock was formed in a marine carbonate-rich environment under sulphate-reducing conditions (Al-Ameri et al., 2013; Sachsenhofer et al., 2015). The similarities in the variety of biomarkers and carbon isotopic compositions of the Middle Jurassic Sargelu source rock and analysed oils (Figs. 5 and 7) are consistent with a genetic relationship.

Stratigraphically, the Cretaceous and Tertiary reservoir rocks hosting the analysed oils directly overly the Middle Jurassic Sargelu source rock (Fig. 2) and therefore, it is very likely that the oils were generated and expelled from this source rock into the Cretaceous and Tertiary reservoir rocks through faults in the southern part of Zagros Fold Belt (Al-Ahmed, 2006).
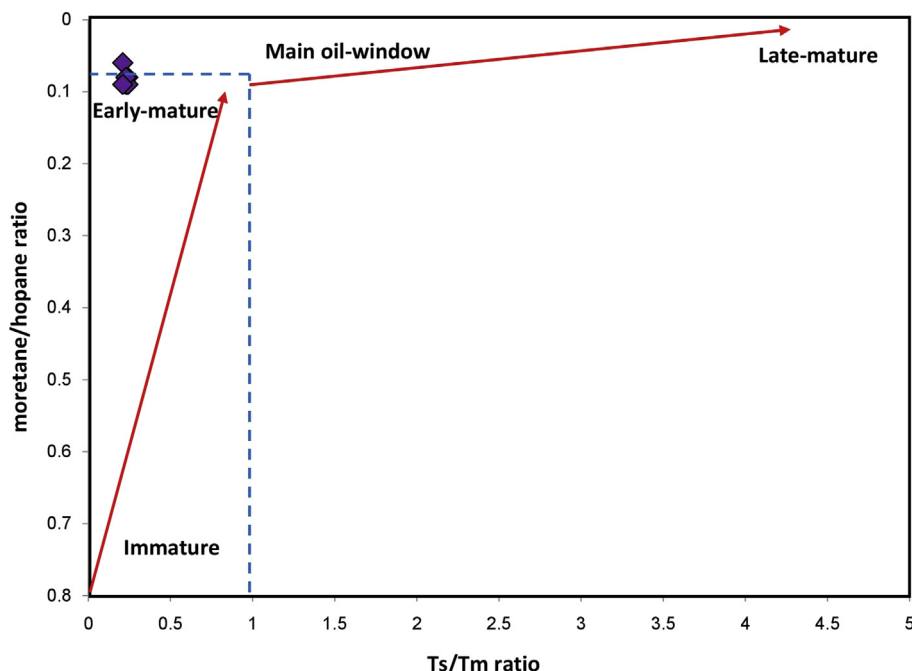
Fig. 13. A range of thermal maturity based on biomarker maturity ratios i.e., Ts/Tm versus moretane/hopane ratios (interpretation based on Mackenzie et al. (1980) and Seifert and Moldowan (1986)).

5. Conclusions

A geochemical investigation of a number of crude oils in the southern Zagros Fold Belt, Iraq suggests the following:

1 There are no significant differences in the oil samples based on the non-biomarker and biomarker geochemical results; therefore, all oils are generated from a common source or sources.
2 The oils are characterized by relatively low API gravity, high sulphur contents, indicating heavy oils generated from a sulphur-rich source rock (Type II-S).
3 The biomarker characteristics of *n*-alkanes, regular isoprenoids, terpanes and steranes suggest that the oils were generated predominantly from a carbonate source rock that received an abundance of marine-derived organic matter (plankton/algal and microorganisms). This is also confirmed by the carbon isotopic compositions of their saturated and aromatic hydrocarbon fractions.
4 Sulphate-reducing conditions within a high salinity stratified setting during deposition of the source rock is supported by low Pr/Ph ratios, high elemental V/Ni ratios, high C_{35} homohopane index values, and the presence of gammacerane.
5 Low values of biomarker maturity parameters and relatively low API gravity and high sulphur contents indicate that the analysed oils were generated from an early-mature source rock.
6 The characteristics of the analysed oils are consistent with their sourcing from the Middle Jurassic- Sargelu carbonate source rock present in the southern part of the Zagros Fold Belt as described by Al-Ameri et al. (2013) and Sachsenhofer et al. (2015).

Appendix A. Peak assignments for alkane hydrocarbons in the gas chromatograms of saturated fractions in the m/z 191 (I) and 217 (II) mass fragmentograms

(I) Peak no.	Compound	Abbreviation
Ts	18α(H),22,29,30-trisnorneohopane	C_{27} Ts
Tm	17α(H),22,29,30-trisnorhopane	C_{27} Tm
29	17α,21β(H)-nor-hopane	C_{29} nor-hopane
30	17α,21β(H)-hopane	C_{30} hopane
29M	17β(H),21α(H)-hopane (moretane)	C_{29}Mor
30M	17 β,21α (H)-Moretane	C_{30}Mor
31S	17α,21β(H)-homohopane (22S)	C_{31}(22S)
31R	17α,21β(H)-homohopane (22R)	C_{31}(22R)
32S	17α,21β(H)-homohopane (22S)	C_{32}(22S)
32R	17α,21β(H)-homohopane (22R)	C_{32}(22R)
33S	17α,21β(H)-homohopane (22S)	C_{33}(22S)
33R	17α,21β(H)-homohopane (22R)	C_{33}(22R)
34S	17α,21β(H)-homohopane (22S)	C_{34}(22S)
34R	17α,21β(H)-homohopane (22R)	C_{34}(22R)
35S	17α,21β(H)-homohopane (22S)	C_{35}(22S)
35R	17α,21β(H)-homohopane (22R)	C_{35}(22R)
(II) Peak no.		
a	13β,17α(H)-diasteranes 20S	C_{27}, C_{29} Diasteranes
b	13β,17α(H)-diasteranes 20R	C_{27}, C_{29} Diasteranes
c	13α,17β(H)-diasteranes 20S	C_{27} Diasteranes
d	13α,17β(H)-diasteranes 20R	C_{27} Diasteranes
e	5α,14α(H), 17α(H)-steranes 20S	C_{29} ααα20S
f	5α,14β(H), 17β(H)-steranes 20R	C_{29} αββ20R
g	5α,14β(H), 17β(H)-steranes 20S	C_{29} αββ20S
h	5α,14α(H), 17α(H)-steranes 20R	C_{27}, C_{28}, C_{29} ααα20R

References

Al-Ahmed, A.A., 2006. Organic Geochemistry, Palynofacies and Hydrocarbon Potential of Sargelu Formation (Middle Jurassic) Northern Iraq. Ph.D. Thesis. University of Baghdad (Unpublished).

Al-Ameri, T.K., Zumberge, J., 2012. Middle and upper Jurassic hydrocarbon potential of the Zagros Fold Belt, north Iraq. Mar. Petroleum Geol. 36, 13—34.

Al-Ameri, T.K., Najaf, A.A., Al-Khafaji, A.S., Zumberge, J., Pitman, J., 2013. Hydrocarbon potential of the Sargelu Formation, north Iraq. Arabian J. Geoscience. http://dx.doi.org/10.1007/s12517-013-0875-8.

Al-Juboury, A., McCann, T., 2008. The Middle Miocene Fatha (lower Fars) formation, Iraq. GeoArabia 13 (3), 141—174.

Al-Sakini, J.A., 1992. Summary of Petroleum Geology of Iraq and the Middle East. Northern Oil Company Press, Kirkuk, 179 pp. (in Arabic).

Aqrawi, A.A.M., Goff, J.C., Horbury, A.D., Sadooni, F.N., 2010. The Petroleum Geology of Iraq, first ed. (Beaconsfield, United Kingdom).

Bally, A.W., Snelson, S., 1980. Realms of subsidence. In: Miall, A.D. (Ed.), Facts and Principles of World Petroleum Occurrence, vol. 6. Canadian Society of Petroleum Geologists Memoir, pp. 9—94.

Barwise, A.J.G., 1990. Role of nickel and vanadium in petroleum classification. Energy Fuels 4, 647—652.

Baskin, D.K., Peters, K.E., 1992. Early generation and characteristics of a sulfur-rich Monterey kerogen. Am. Assoc. Petroleum Geol. Bull. 76, 1—13.

Boreham, C.J., Hope, J.M., Hartung-Kagi, B., 2001. Understanding source, distribution and preservation of Australian natural gas: a geochemical perspective. Aust. Prod. Petroleum Explor. Assoc. J. 41, 523—547.

Brassell, S.C., Eglinton, G., Maxwell, J.R., Philp, R.P., 1978. Natural background of alkanes in the aquatic environment. In: Hutzinger, O., van Lelyveld, L.H., Zoeteman, B.C.J. (Eds.), Aquatic Pollutants: Transformation and Biological Effects. Pergamon, Oxford, pp. 69—86.

Bray, E.E., Evans, E.D., 1961. Distribution of n -paraffins as a clue to recognition of source beds. Geochimica et Cosmochimica Acta 22, 2—15.

Buday, T., 1980. The Regional Geology of Iraq, Stratigraphy and Palaeogeography, 455 pages. State Organization for Minerals, Baghdad. Iraq.

Chandra, K., Mishra, C.S., Samanta, U., Gupta, A., Mehrotra, K.L., 1994. Correlation of different maturity parameters in the Ahmedabad—Mehsana block of the Cambay basin. Org. Geochem. 21, 313—321.

Clark, J.P., Philp, R.P., 1989. Geochemical characterization of evaporate and carbonate depositional environments and correlation of associated crude oils in the Black Creek Basin, Alberta. Bull. Can. Petroleum Geol. 37, 401—416.

Collister, J.W., Wavrek, D.A., 1996. ^{13}C compositions of saturate and aromatic fractions of lacustrine oils and bitumens: evidence for water column stratification. Org. Geochem. 24, 913—920.

Cranwell, P.A., 1977. Organic geochemistry of Cam Loch (Sutherland) sediments. Chem. Geol. 20, 205—221.

Didyk, B.M., Simoneit, B.R.T., Brassell, S.C., Eglinton, G., 1978. Organic geochemical indicators of palaeoenvironmental conditions of sedimentation. Nature 272, 216—222.

Dunington, H.V., 1958. Generation, migration, accumulation and dissipation of oil in Northern Iraq. In: Weeks, G.L. (Ed.), Habitat of Oil. The American Association of Petroleum Geologists, pp. 1194—1251.

Ekweozor, C.M., Telnaes, N., 1990. Oleanane parameter: verification by quantitative study of the biomarker occurrence in sediments of the Niger Delta. Org. Geochem. 16, 401—413.

El-Gayar, M.S., Mostafa, A.R., Abdelfattah, A.E., Barakat, A.O., 2002. Application of geochemical parameters for classification of crude oils from Egypt into source related types. Fuel Process. Technol. 79, 13—28.

El Nady, M.M., Harb, F.M., Mohamed, N.S., 2014. Biomarker characteristics of crude oils from Ashrafi and GH oilfields in the Gulf of Suez, Egypt: an implication to source input and paleoenvironmental assessments. Egypt. J. Petroleum 23, 455—459.

Galarraga, F., Reategui, K., Martínez, A., Martínez, M., Llamas, J.F., Marquez, G., 2008. V/Ni ratio as a parameter in palaeoenvironmental characterisation of non mature medium-crude oils from several Latin American basins. J. Pet. Sci. Eng. 61, 9—14.

Gransch, J.A., Posthuma, J., 1974. On the origin of sulfur in crudes. In: Tissot, B., Bienner, F. (Eds.), Advances of Organic Geochemistry. Editions Technip, Paris, pp. 727—739.

Hakimi, M.H., Abdullah, W.H., Shalaby, M.R., 2011. Organic geochemical characteristics of crude oils from the Masila Basin, eastern Yemen. Org. Geochem. 42, 465—476.

Haq, B.U., 1980. Introduction to Marine Micropaleontology. Elsevier, New York, 376pp.

Huang, W.Y., Meinschein, W.G., 1979. Sterols as ecological indicators. Geochimica et Cosmochimica Acta 43, 739—745.

Huang, H., Pearson, M.J., 1999. Source rock palaeoenvironments and controls on the distribution of dibenzothiophenes in lacustrine crude oils, Bohai Bay Basin, Eastern China. Org. Geochem 30, 1455—1470.

Hunt, J., 1996. Petroleum Geochemistry and Geology. W.H. Freeman and Company, New York, USA, 743 pp.

Jassim, S.Z., Goff, C., 2006. Geology of Iraq. Dolin, Prague and Moravian Museum, Brno, 341 pp.

Kent, Norman, 2010. Structure of the Kirkuk embayment, northern Iraq: foreland structures or Zagross Fold Belt structures. GeoArabia 15 (4), 147—188.

Larter, S.R., Head, I.M., Huang, H., Bennett, B., Jones, M., Aplin, A.C., Murray, A., Erdmann, M., Wilhelms, A., di Primio, R., 2005. Biodegradation, gas destruction and methane generation in deep subsurface petroleum reservoirs: an overview. In: Dore, A.G., Vining, B. (Eds.), Petroleum Geology: Northwest Europe and Global Perspectives: Proceedings of the 6th Petroleum Geology Conference. Geological Society, London, pp. 633—640.

Lewan, M.D., 1984. Factors controlling the proportionality of vanadium to nickel in crude oils. Geochim. Cosmochim. Acta 48, 2231—2238.

Mackenzie, A.S., Patience, R.L., Maxwell, J.R., Vandenbroucke, M., Durand, B., 1980. Molecular parameters of maturation in the Toarcian shales, Paris Basin, France. Changes in the configuration of acyclic isoprenoids alkanes, steranes and triterpanes. Geochimica et Cosmochimica Acta 44, 1709—1721.

Markovaa, K., Stefanovab, M., Milakovskac, Z., Marinovb, S.P., 2016. A comparison of black claystones, lignites and dump materials from the Maritsa Iztok Coal Basin, Bulgaria, using organic geochemical proxies. Chem. Erde — Geochem. 76 (3), 405—417.

Mohialdeen, I.M.J., 2007. Stratigraphy and sedimentology of organic rich limestones of the Chia Gara Formation, Rania area, Sulaimani, Kurdistan region, NE Iraq. J. Zankoy Sulaimani 10A, 91—102.

Mohialdeen, I.M.J., Hakimi, M.H., Al-Beyati, F.M., 2013. Geochemical and petrographic characterization of late Jurassic-early Cretaceous Chia Gara Formation in northern Iraq: palaeoenvironment and oil-generation potential. Mar. Petroleum Geol. 43, 166—177.

Moldowan, J.M., Sundararaman, P., Schoell, M., 1985. Sensitivity of biomarker properties to depositional environment and/or source input in the Lower Toarcian of S.W. Germany. Org. Geochem. 10, 915—926.

Peters, K.E., Fowler, M.G., 2002. Applications of petroleum geochemistry to exploration and reservoir management. Org. Geochem. 33, 5—36.

Peters, K.E., Walters, C.C., Moldowan, J.M., 2005. The Biomarker Guide: Biomarkers and Isotopes in Petroleum Exploration and Earth History, , second ed.vol. 2. Cambridge University Press, Cambridge.

Philp, R.P., 1985. Biological markers in fossil fuel production. Mass Spectrom. Rev. 4, 1—54.

Powell, T.G., McKirdy, D.M., 1973. Relationship between ratio of pristane to phytane, crude oil composition and geological environment in Australia. Nat. Phys. Sci. 243, 37—39.

Roushdy, M.I., El Nady, M.M., Mostafa, Y.M., El Gendy, N.S., Ali, H.R., 2010. Biomarkers characteristics of crude oils from some oilfields in the Gulf of Suez, Egypt. J. Am. Sci. 6, 911—925.

Sachsenhofer, R.F., Bechtela, A., Gratzera, R., Rainerb, T.M., 2015. Source-rock maturity, hydrocarbon potential and oil-source rock correlation in well Shorish-1, Erbil province, Kurdistan Region, Iraq. J. Petroleum Geol. 38, 357—382.

Sadooni, F.N., 1993. Stratigraphic sequence, microfacies, and petroleum prospects of the Yamama formation, lower cretaceous, southern Iraq. Am. Assoc. Petroleum Geol. Bull. 77, 1971—1988.

Sadooni, F.N., Aqrawi, A.M., 2000. Cretaceous Sequence Stratigraphy and Petroleum Potential of the Mesopotamian Basin, Iraq. Special Publication 69. Society for Sedimentary Geology, ISBN 1-56576-075-1, pp. 315—334.

Seifert, W.K., Moldowan, J.M., 1978. Application of steranes, terpanes and monoaromatic to the maturation, migration and source of crude oils. Geochimica et Cosmochimica Acta 42, 77—95.

Seifert, W.K., Moldowan, J.M., 1981. Palaeoreconstruction by biological markers. Geochimica et Cosmochimica Acta 45, 783—794.

Seifert, W.K., Moldowan, J.M., 1986. In: Johns, R.B. (Ed.), Use of Biological Markers in Petroleum Exploration, vol. 24. Methods in Geochemistry and Geophysics Book Series, Amsterdam, pp. 261—290.

Sinninghe Damsté, J.S., Kenig, F., Koopmans, M.P., Koster, J., Schouten, S., Hayes, J.M., de Leeuw, J.W., 1995. Evidence for gammacerane as an indicator of water column stratification. Geochim. Cosmochim. Acta 59, 1895—1900.

Sofer, Z., 1984. Stable carbon isotope compositions of crude oils: application to source depositional environments and petroleum alteration. Am. Assoc. Petroleum Geol. Bull. 68, 31—49.

Summons, R.E., Thomas, J., Maxwell, J.R., Boreham, C.J., 1992. Secular and environmental constraints on the occurrence of dinosterane in sediments. Geochimica et Cosmochimica Acta 56, 2437—2444.

ten Haven, H.L., Rohmer, M., Rullkotter, J., Bisseret, P., 1989. Tetrahymanol, the most likely precursor of gammacerane, occurs ubiquitously in marine sediments. Geochim. Cosmochim. Acta 53, 3073—3079.

Tissot, B.P., Welte, D.H., 1984. Petroleum Formation and Occurrence, second ed. Springer Verlag, Berlin, p. 699.

van Bellen, Van, R.C., Dunnington, H.V., Wetzel, R., Morton, D.M., 1959. Lexique Stratigraphquie International, Vol. III. Asie, Fasicule 10a Iraq, 333 pages. Centre National de la Recherche Scientifique.

Waples, D.W., Machihara, T., 1991. Biomarkers for Geologists: a Practical Guide to the Application of Steranes and Triterpanes in Petroleum Geology. AAPG Methods in Exploration Series, No. 9. The American Association of Petroleum Geologists, Tulsa, Oklahoma 74101, USA.

Wenger, L.M., Davis, C.L., Isaksen, G.H., 2002. Multiple controls on petroleum biodegradation and impact on oil quality. Reserv. Eval. Eng. 375—383.